Inorganic Chemistry

ARTICLE

pubs.acs.org/IC

Iron(II) Binding to Amyloid-β, the Alzheimer's Peptide

Fatima Bousejra-ElGarah, Christian Bijani, Yannick Coppel, Peter Faller,* and Christelle Hureau*

CNRS, LCC (Laboratoire de Chimie de Coordination), 205 route de Narbonne, F-31077 Toulouse, France

Université de Toulouse, UPS, INPT, LCC, F-31077 Toulouse, France

Supporting Information

ABSTRACT: Iron has been implicated in Alzheimer's disease, but until now no direct proof of Fe^{II} binding to the amyloid-β peptide (Aβ) has been reported. We used NMR to evidence Fe^{II} coordination to full-length Aβ40 and truncated Aβ16 peptides at physiological pH and to show that the Fe^{II} binding site is located in the first 16 amino-acid residues. Fe^{II} caused selective broadening of some NMR peaks that was dependent on the Fe:Aβ stoichiometry and temperature. Analysis of Fe^{II} broadening effect in the ^{1}H, ^{13}C, and 2D NMR data established that Asp1, Glu3, the three His, but not Tyr10 nor Met35 are the residues mainly involved in Fe^{II} coordination.

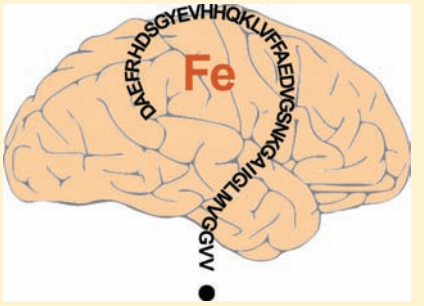

INTRODUCTION

Iron is an essential micronutrient involved in many fundamental processes including dioxygen transport and electron transfer reactions. Hence, its dysregulation is at the origin of several diseases. The brain is the second Fe-richest organ (after the liver) and contains about 60 mg of nonheme Fe. This Fe content increases with age. Fe accumulation has been linked to many neurological diseases, including Parkinson's disease, Huntington's disease, and Alzheimer's disease (AD), and is observed in brain regions associated to decreased function and cell loss (ref 1 and references therein).

In AD, Fe overload has been localized in senile plaques (SP) and neurofibrillary tangles, two hallmarks of AD patients brains, and in neuropils.[2] The SP mainly consist of a 39−43 residue peptide called amyloid-β (Aβ) in aggregated states and contain abnormally high (~mM) Fe, Cu, and Zn concentrations.[3] This Fe connected to SP has been proposed to originate mainly from ferritin or related iron−oxide particles.[4,5] However, histochemical studies indicated that some Fe could also be bound directly to Aβ[2] in line with the colocalization of aggregated Aβ and Fe within the SP.[6] This Fe might be released (from ferritin) under pathological conditions.[1,4]

In AD as in other diseases, Fe toxicity may be due to the propensity of the ferrous state to generate reactive oxygen species (ROS) via Fenton- or Haber−Weiss-type reactions.[7,8] In this context, it has been proposed that Aβ decreases Fe-induced oxidative stress.[9] On the contrary, a deleterious effect due to Fe involvement in Aβ aggregation has been reported.[10,11] Lastly, Fe concentration affects indirectly the production of Aβ as its precursor protein (APP) has an active iron-responsive element,[12,13] and recently evidence for ferroxidase activity of APP was reported.[14] Hence, there is diverse evidence for the roles played by Fe in AD (also reviewed in ref 15), but it is still not clear if Fe binds to Aβ directly. Thus, better disentangling the chemistry of Fe ions at the molecular level is of paramount importance to progress in the knowledge of Fe roles in AD.

In vitro studies regarding the interactions of Cu and Zn ions with Aβ peptides have generated great interest in the last few years, and a multitude of articles dealing with coordination of Cu^{II}, Zn^{II}, and to a lesser extent Cu^{I} to the N-terminal portion of the full-length Aβ peptides (namely, the Aβ16 peptide) have been published over the past decade (reviewed in ref 16). Indeed, several frozen solution studies revealed that the Aβ16 peptide is a valid model for coordination of the metal ions to the full-length peptide.[17−19] A consensus exists for the binding site of the Cu^{II}−Aβ species predominant at physiological pH (and usually noted component I; refs 20 and 21 and references therein) and for the Cu^{I}−Aβ complex[22,23] but not for the second minor Cu^{II}−Aβ species and for Zn^{II}−Aβ.

NMR is a powerful technique to determine metal-ion binding sites in fluid solution and was used to investigate coordination of Cu^{II} and Zn^{II} to the full-length Aβ via assessing line broadening.[24,25] In $^{1}H-^{13}C$ experiments, it was evidenced that the Zn^{II} binding site is in the Aβ16 fragment.[24] By $^{1}H-^{15}N$ correlation experiments, it was proposed that Cu^{II} first anchors to the His residues (at positions 6, 13, and 14) and then binds to less precise sites than in shorter model peptides. However, in $^{1}H-^{15}N$ experiments the signals of potential ligands are affected by an exchange process with the solvent and are missing in the peptide spectrum (before addition of metal ions), thus precluding a straightforward analysis of metal-ion binding sites.[25] This is the reason why detailed analysis were also performed by ^{1}H, ^{13}C, and $^{1}H-^{13}C$ correlation experiments on Aβ16 peptides.[26,27]

Received: June 9, 2011
Published: July 29, 2011

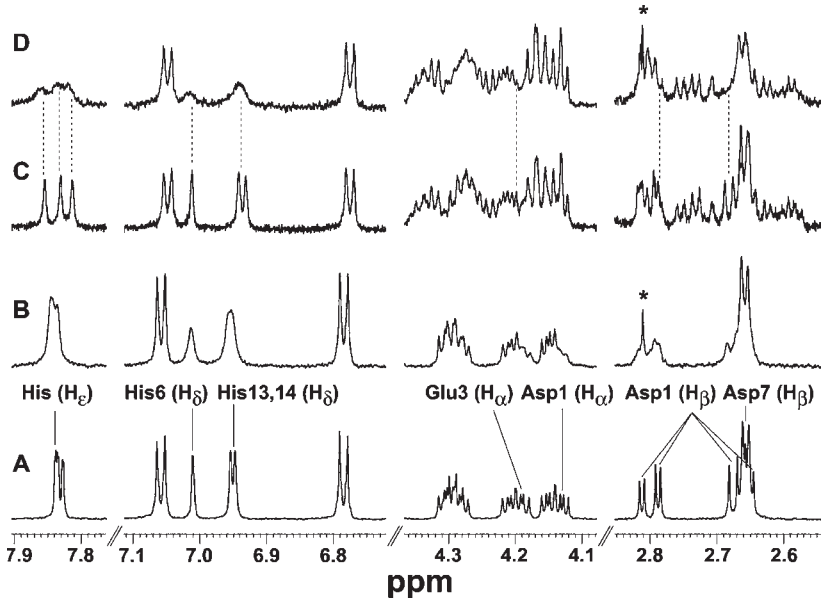

Figure 1. ^{1}H NMR spectra of 0.2 mM Aβ16 (A, B) and 0.2 mM Aβ40 (C, D) peptides in 0.04 M phosphate buffer/D_2O and in the absence (A, C) and presence (B, D) of 0.3 equiv of Fe^{II}, pH = 7.2, T = 298K, ν = 700 MHz. Asterisk (*) is from added DFO.

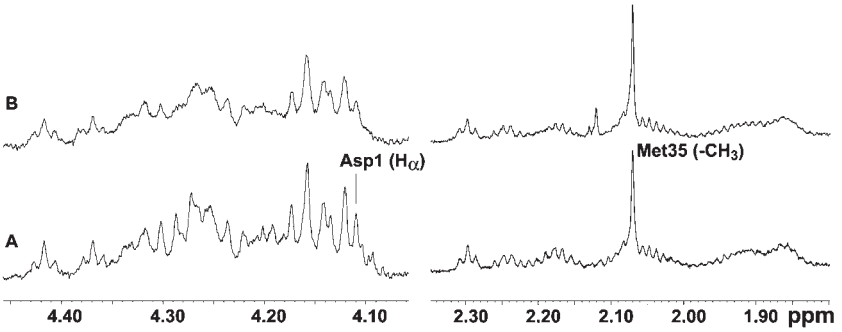

Figure 2. ^{1}H NMR spectra of 0.2 mM Aβ peptides in 0.04 M phosphate buffer/D_2O. (Left) Zoom on the H_α region of the Aβ40 peptide: (A) without Fe^{II}, (B) with 0.3 equiv of Fe^{II}. Recording conditions: pH = 7.4, T = 298 K, ν = 500 MHz. Note that to better detect the Fe^{II}-induced broadening effect on the Asp1-H_α on the Aβ40 peptide, we recorded it at a slightly higher pH than in usual conditions. (Right) Zoom on the $-CH_3$ from Met 35 in the Aβ40 peptide: (A) without Fe^{II}, (B) with 0.3 equiv of Fe^{II}. Recording conditions: pH = 7.2, T = 298 K, ν = 700 MHz.

In contrast to Cu and Zn, to the best of our knowledge, no data on Fe binding to Aβ has been reported. The few studies available focused on oxidized state Fe^{III} and report the effect of Fe^{III} on Aβ aggregation[10,28,29] and Aβ modulation of Fe ROS production,[30−32] but it seems that Aβ binds Fe^{III} not strong enough to avoid Fe precipitation.[29] Thus, direct interaction between Fe and Aβ has still to be demonstrated. As the brain is a rather reducing environment and because production of ROS involves the reduced ions Fe^{II} (and Cu^{I}), study of the ferrous ion is of biological relevance and Fe^{II} might interact more specifically with Aβ than Fe^{III}. Here, ^{1}H, ^{13}C, and 2D NMR experiments were carried out to obtain straightforward indications of Fe^{II} coordination to Aβ and to propose a Fe^{II} binding motif.

RESULTS

^{1}H NMR Data on Fe^{II} Interaction with Aβ40 and Aβ16. Full-length Aβ40 at low concentration (200 μM) to minimize aggregation and Aβ16 peptides was measured by ^{1}H NMR, and the effect of addition of Fe^{II} under anaerobic condition (see Experimental Section for details) was compared. For both peptides the H_δ and H_ε imidazoles protons, the two diastereotopic H_β protons of Asp1 (Figure 1), the H_α of Asp1 (Figure 2, left), and to a lesser extent the H_α of Glu3 are selectively and significantly broadened upon addition of Fe^{II}. No strong broadening of residues in the stretch 17−40 could be detected (see also Figure S1, Supporting Information), including the well-resolved resonance of the potential ligand Met35 (Figure 2, right). The diastereotopic H_β protons of Asp23 detected at ∼2.76 and 2.62 ppm (Figure 1) are not broadened as well as those of Ala21 (Figure S2, Supporting Information), the closest residue of Glu22, the third potential ligand present in the 17−40 fragment, which cannot be unambiguously observed in the ^{1}H spectrum. This strongly indicates that the principal Fe^{II} binding site is confined to Aβ16, the N-terminal portion of Aβ40 (as is the case for Cu^{II} and Zn^{II}). Furthermore, Aβ40 has the propensity to aggregate, which is enhanced by treatment for anaerobic conditions (see Experimental Section), lowering pH, and higher temperature. Aggregation leads to line broadening and thus precludes investigation of the Fe^{II} binding to soluble Aβ40 by

dx.doi.org/10.1021/ic201233b |Inorg. Chem. 2011, 50, 9024–9030

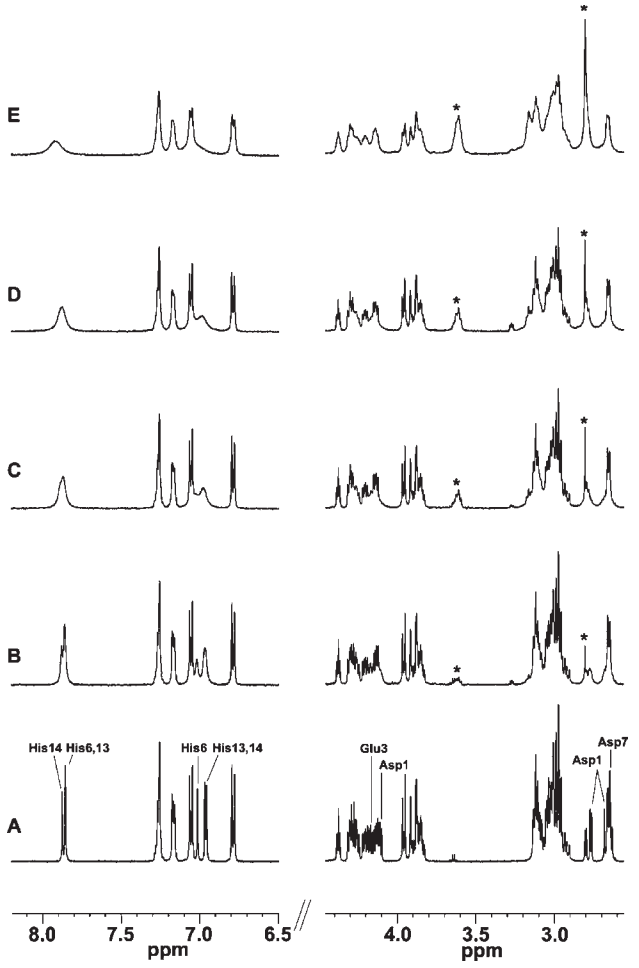

Figure 3. Regions of interest in the ^{1}H NMR spectra of 1 mM Aβ16 peptide in 0.2 M phosphate buffer/D_2O (A) and in the presence of 0.1 (B), 0.3 (C), 0.5 (D), and 1.0 (E) equiv of Fe^{II}, pH = 7.2, T = 298 K, ν = 500 MHz. Asterisk (*) is from added DFO.

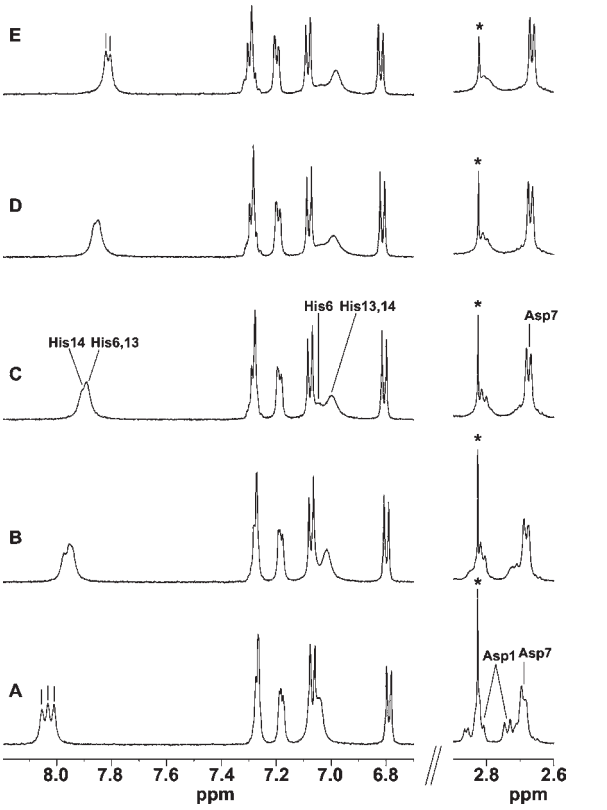

Figure 4. ^{1}H NMR spectra of 1 mM Aβ16 peptide in 0.2 M phosphate buffer/D_2O and in the presence of 0.3 equiv of Fe^{II} at 278 (A), 288 (B), 298 (C), 308 (D), and 318 K (E), pH_{298K} = 7.2, ν = 500 MHz. Asterisk (*) is from added DFO.

long-lasting ^{13}C and 2D experiments and pH-dependent or temperature studies. Consequently, further experiments were performed on the Aβ16 peptide.

Fe^{II} to Aβ Titration Experiments. The Fe^{II} to Aβ stoichiometry dependence of the ^{1}H NMR signals is exemplified in Figure 3, which shows the aromatic region and a selected portion of the aliphatic region. Note that the broadening effect observed in Figure 1 (spectrum B) and 3 (spectrum C) cannot be directly compared due to different recording conditions: at 700 MHz and [Aβ] = 0.2 mM and at 500 MHz and [Aβ] = 1 mM, respectively. The H_δ ($\delta \approx 6.9$ ppm) and H_ε ($\delta \approx 7.8$ ppm) imidazole protons as well as the H_α and two diastereotopic H_β protons of Asp1 are selectively broadened and up-shifted upon increasing addition of Fe^{II}. The rest of the spectrum remains mainly unchanged. However, at Fe:Aβ stoichiometry higher than 0.5, broadening becomes less specific and it is then difficult to correctly discriminate which residues are mainly affected by Fe addition. This is likely due to precipitation of a very small fraction of Fe as hydroxide that disturbed the spectrum, and this is the reason why experiments were performed at Fe:Aβ stoichiometry of 0.3. Furthermore, as no strong hyperfine shift typical of well-defined and tight Fe binding was observed (Figures 1−3), the NMR signals were quantified via the internal standard 4,4-dimethyl-4-silapentane-1-sulfonic acid before and after Fe^{II} addition to ensure that no significant loss of Aβ16 protons occurred. Indeed, as shown in Figure S3, Supporting Information, all Aβ16 proton resonances remained in the classical proton chemical shift range, contrary to what is observed in the case of tight binding of high-spin Fe(II) to proteins or ligands, where chemical shifts can undergo considerable change. These first observations are fully consistent with other NMR studies on Fe^{II} binding to proteins[33,34] or DNA[35] with moderate affinity and/or flexible binding.

Temperature Dependence Experiments. To disentangle the origins of the Fe^{II}-induced selective effects of the NMR signals, a temperature dependence study was performed (Figure 4 and Figure S4, Supporting Information, for the full spectra). The first effect of temperature is a modification in the chemical shift of the His protons. This shift is attributed to a decrease of the His pK_a values with the increase of the temperature,[36] the pH value of the phosphate buffer being mainly independent of the temperature. To verify that broadening was not dependent on the His protonation state, we recorded ^{1}H NMR spectra of Aβ16 in the presence of 0.3 equiv of Fe^{II} at pH 6.9 and 7.5 (Figure S5, Supporting Information). At the former pH value (298 K), the His protonation state is equivalent to that obtained at pH 7.2 and T = 278K, while at the latter pH value (298 K), the His protonation state is equivalent to that obtained at pH 7.2 and T = 318 K. This study evidences that pH has very little influence on the broadening and thus indicates that the effects observed in the temperature dependence experiment are attributable to a change in the temperature only (and not to a resulting change the protonation state of the His).

dx.doi.org/10.1021/ic201233b |*Inorg. Chem.* 2011, 50, 9024–9030

Hence, temperature induces strong modification in the broadening observed on His H_ε and H_δ and Asp1 H_α and H_β protons. Broadening has mainly two origins: PRE (paramagnetism relaxation enhancement) due to the high-spin Fe^{II} (d^6, $S = 2$) and chemical exchange. (i) PRE diminishes with distance by a power of 6 and will mainly affect atoms in close vicinity of the metal center, similar to what is observed in the Cu^{II} case.[26] In the case of a dynamical binding as encountered in the present system, broadening is expected to increase with an increase in temperature.[37,38] This is linked to the increase of k_{off} at higher temperature.[37,38] Furthermore, motion of the paramagnetic center with respect to the ligand will also reduce the pseudocontact shift. This is the reason why only very small chemical shifts are observed, which are likely due to chemical exchange more than to paramagnetism. (ii) Exchange between two chemically different states of apo- and holo-peptides (conformations, protonation states...) will also affect atoms in metal center coordination as detected by ^1H NMR for the diamagnetic Cu^{I} [22] and Zn^{II} or Cd^{II}.[39] In that case, broadening is expected to decrease with an increase in temperature. For the Fe^{II}—Aβ16 system, a combination of PRE and of chemical exchange is observed. Indeed, when the temperature is increased from 278 to 298 K, peaks of the Fe^{II}-responsive residues become broader. This is attributed to PRE effect. However, when the temperature is increased from 298 to 318 K (above 318 K the sample evolves significantly), Fe^{II}-responsive features tend to become sharper again, in line with the chemical exchange effect becoming preponderant over the PRE effect. A very interesting point is that two residue families could be distinguished: the first one (His13 and His14) for which the peak narrowing upon temperature increase between 298 and 318 K is strong, and the second one (His6 and Asp1) for which it is less important. This strongly suggests that the two broadening effects impact differently the His13-His14 diad compared to Asp1 and His6 residues. This is tentatively attributed to either a stronger PRE effect on Asp1 and His6 residues and/or a slower chemical exchange for Asp1-His6 fragment compared to the rest of the peptide, including His13 and His14.

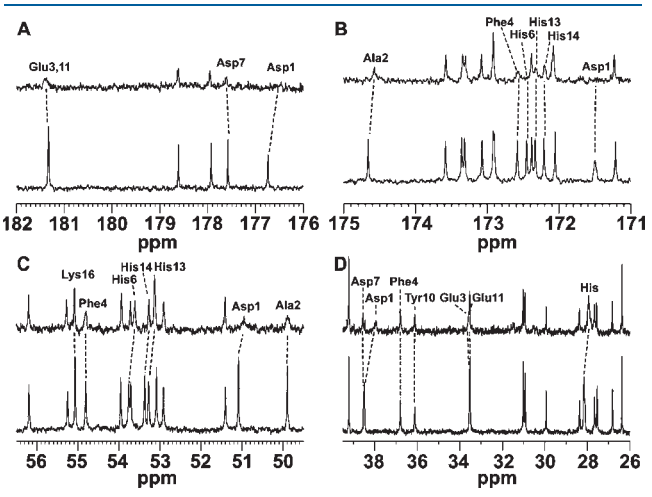

Figure 5. COO^- (A), CO (B), C_α (C), and $C_{\beta,\gamma}$ (D) regions of the $^{13}C\{1H\}$ NMR spectra of Aβ16 peptide in 0.2 M phosphate buffer/D_2O (bottom spectrum in each panel) and in the presence of 0.3 equiv of Fe^{II} (top spectrum in each panel), pH 7.2, $T = 298$ K, $\nu = 128.5$ MHz.

^{13}C and 2D Experiments. To complete the ^1H NMR data, ^{13}C and 2D data were recorded at 298 K and in the presence of 0.3 equiv of Fe^{II}. These conditions lead to the most effective discrimination between peaks undergoing different broadening amplitude. Figure 5 shows the impact of Fe^{II} addition to the ^{13}C signals. The Asp1 and to a lesser extent the Asp7 and Glu $COO^{-13}C$ nuclei are broadened. His6 and Asp1 ^{13}CO fully vanish, while those of Ala2, Phe4, His13, and His14 are less affected but still strongly broadened. Regarding C_α, those of Asp1 and to a lesser extent of Ala2 and Phe4 are broadened while those of the three His residues are shifted but not affected by broadening. The C_β and C_γ atoms are less affected with the exception of the Asp1 C_β. The aromatic ^{13}C mostly broadened are those of the three His with a slightly weaker broadening observed for C_ε (Figure S6, Supporting Information).

Figure 6 shows that the H_δ—C_δ (7.0 ppm; 117 ppm), H_ε—C_ε (7.8 ppm; 136 ppm), and H_β—C_β (3.1 ppm; 28 ppm) correlation peaks of the His residues disappeared after addition of 0.3 equiv of Fe^{II}, while the His H_α—C_α (4.5 ppm; 53 ppm) correlation peaks are shifted. The Asp1 H_α—C_α (4.1 ppm; 51 ppm), H_β—C_β (2.7 ppm; 39 ppm), Glu3 H_γ—C_γ (2.2 ppm; 34 ppm), and Ala H_α—C_α (4.3 ppm; 50 ppm) correlation peaks also disappeared after addition of 0.3 equiv of Fe^{II}.

Information collected from the ^1H, ^{13}C, and 2D NMR data (see also Figures S7 and S8, Supporting Information) is gathered in Scheme 1, in which the broadening and shift of relevant (CH) positions are recapitulated. At 298 K, the residues mainly affected

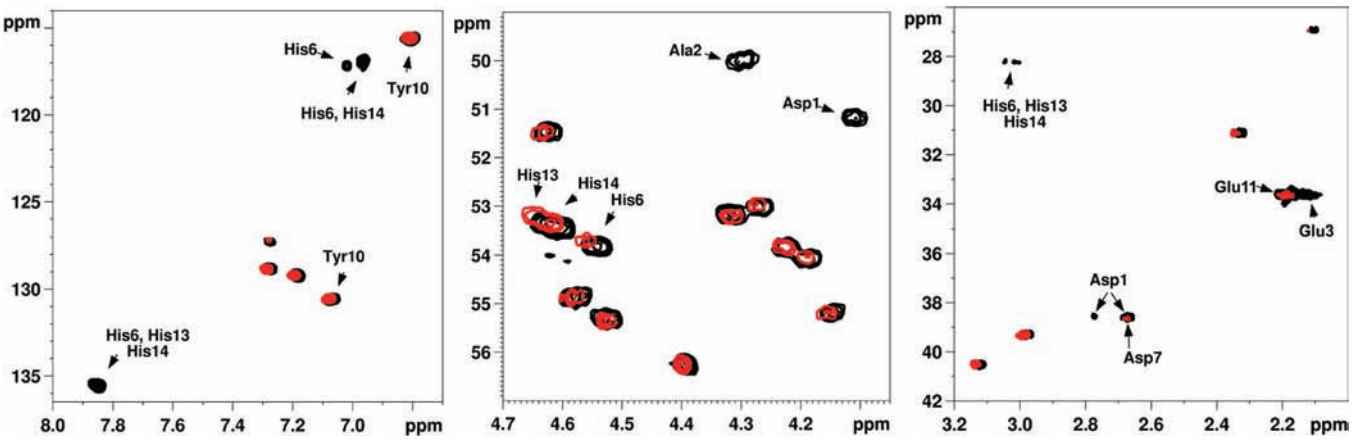

Figure 6. 2D ^1H—^{13}C HSQC of 5 mM Aβ16 peptide (black) and 2 mM Aβ16 peptide in presence of 0.3 equiv of Fe^{II} (red) in 0.2 M phosphate buffer/D_2O at pH 7.2, $T = 298$ K, $\nu = 500$ MHz. (Left) Aromatic regions, (middle) (C_α ; H_α) regions, and (right) ($C_{\beta,\gamma}$; $H_{\beta,\gamma}$) regions.

dx.doi.org/10.1021/ic201233b |*Inorg. Chem.* 2011, 50, 9024–9030

Scheme 1. Schematic Representation of the Most Affected $-(CH_n)-$ Positions in Aβ16[a]

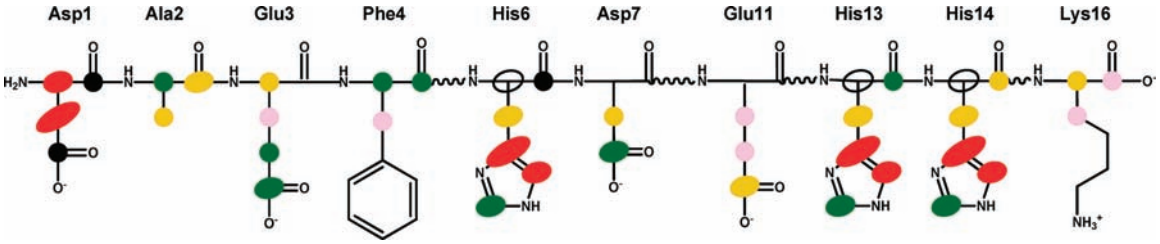

[a] The color code is as follow: black = disappeared, red = highly broadened, green = broadened, orange-yellow = moderately broadened, pale pink = slightly broadened. Ellipsoid code stands for the signal shifting: circle = no shift, small ellipsoid = slight shift, large ellipsoid = significant shift.

Scheme 2. (A) List of the Potential Binding Functions Affected by Cu^{II} (from ref 26) or Fe^{II} (in bold, the mostly broadened residues); (B) Cu^{II} Binding Site in Aβ (component I) and Proposition of Fe^{II} Binding Site

A

	Cu^{II}	Fe^{II}
NH_2	Asp1 (Cα)	Asp1 (Cα)
Im	His6, His13, His14	**His6**, His13, His14
COO^-	Asp1, Glu3, Asp7, Glu11, Lys16 (C-term)	**Asp1,** Glu3, (Asp7)
CO	**Asp1**, His6, His13, His14	**Asp1**, **His6,** His13, His14

B

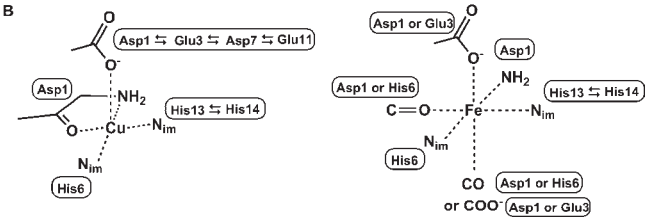

by Fe^{II} addition are the Asp1 and the three His. Among the three remaining carboxylic acids, Glu3 is the one mostly influenced by Fe^{II}. Regarding the CO from His, the one in position 6 is more affected than those in positions 13 and 14.

DISCUSSION

As previously observed for Cu^{II}–Aβ16 complexes,[26,27] Fe^{II} binding to Aβ16 is very dynamic and likely involves several differently populated coordination modes of similar types. As a consensus has been reached in the literature on the nature of the Cu^{II} coordination sphere in component I, a comparison (detailed below) of NMR data obtained on Cu^{II}–Aβ16 component I and Fe^{II}–Aβ16 was used to propose Fe^{II} binding site(s) in Aβ16. Note that since no steric constraints are exerted by the Aβ16 ligand, hexacoordination of the Fe^{II} ion has been assumed. The NMR data are compared in Scheme 2a (and Scheme S2, Supporting Information), and the corresponding Cu^{II} and Fe^{II} binding sites are depicted in Scheme 2b. (i) The α position of Asp1 is affected by both Cu^{II} and Fe^{II}, suggesting that the $-NH_2$ is bound to both metal centers. (ii) The imidazole rings of the three His are all broadened in the presence of Cu^{II} or Fe^{II}. For the Cu^{II}–Aβ16 component I, it has been proposed by other techniques that while His6 is always bound to Cu^{II}, His 13 and His14 are in equilibrium for one binding position. In the Fe^{II} species, the same kind of His binding takes place as indicated by the ^{1}H temperature-dependent study. (iii) As in the Cu^{II} case, the Tyr10 residue was not significantly affected by Fe^{II} and thus its binding was ruled out. (iv) Regarding the carboxylate residues, they were all equivalently affected in the case of Cu^{II}–Aβ16 component I, while in the Fe^{II} case mostly those of Asp1 and Glu3 and to a lesser extent that of Asp7 are broadened. This suggests that both COO^- groups from Asp1 and Glu3 are bound to Fe^{II}, whereas all COO^- groups were in equilibrium for the Cu^{II} apical position. (v) The carbonyl functions of Asp1 were predominantly broadened in the Cu^{II} case, those of Ala2 and of the three His being less affected. In the Fe^{II} case, both CO functions from Asp1 and His6 are significantly more affected than those of Ala2 and His13 and His14. This may be in line with the simultaneous formation of two metallacycles, one with $-NH_2$ (Asp1) and the other with the imidazole ring of His6, instead of only one in Cu^{II}–Aβ16 component I. (vi) It is worth noting that almost all CO and $C_\alpha H_\alpha$ positions in the 1–6 fragment are noticeably broadened by Fe^{II}, a fact that was not observed in the Cu^{II} case. This may indicate that confinement of Fe^{II} in the 1–6 N-terminal part of the Aβ peptide induces constraints on the backbone peptide.

As may not be anticipated based on the different chemical nature of the two Cu^{II} (d^9) and Fe^{II} (d^6) ions, the binding sites of Fe^{II} and of Cu^{II} (component I) are very close, showing only subtle differences that may however impact the aggregation process. Differences are more significant with the metal center binding sites in component II of the Cu^{II}–Aβ species and in the Cu^{I}–Aβ complex, the other reduced redox metal ion of importance (note that Zn^{II} is not discussed since no consensual data are reported in the literature). Indeed, Cu^{I} binds linearly to two out of the three imidazoles moieties of His residues.[22,23] Regarding component II of the Cu^{II}–Aβ species, two main coordination spheres are proposed in the literature: (i) the three imidazole rings and the CO function from the Ala2-Glu3 peptide bond (ref 40 and references therein) or (ii) the NH_2 (Asp1), the deprotonated amidyl from the Asp1-Ala2 bond, the C=O group from Ala2-Glu3, and an imidazole ring from either His6, His13, or His14 (refs 20 and 26 and references therein). Hence, whatever the proposition retained, difference with the Fe^{II} binding site is important. Note that contrary to what is observed for Cu^{II}, no pH dependence of Fe^{II} binding to Aβ was found near physiological pH. This is attributed to a lesser Lewis acidity of Fe^{II} compared to Cu^{II}.

CONCLUDING REMARKS

We reported for the first time a study of Fe^{II} coordination to Aβ at the molecular scale and show that the binding site is confined in the 1–16 N-terminal fragment of the Aβ peptide. We also tentatively proposed a structural binding model consistent with the data presently available. During the course of our study,

dx.doi.org/10.1021/ic201233b |Inorg. Chem. 2011, 50, 9024–9030

we have been confronted with rapid oxidation of Fe^{II} in the presence of Aβ and to its subsequent precipitation. This may explain why Fe was not found copurified with Aβ brain extracts (exposed to dioxygen during measurements) contrary to Cu^{II} and Zn^{II}.[41] This latter result was frequently used to argue against direct interaction between Fe and Aβ in vivo, an analysis which seems worth being reevaluated. Indeed, the first insights of Fe^{II} binding to the amyloid-β peptide showed here might be of biological relevance due to the more reducing environment found in the brain. That such an interaction might occur in vivo is still an open issue. Although beyond the scope of this paper, a more precise determination of the binding affinity is key to better evaluate this question. It will also be of paramount importance to determine how Fe^{II} binding to Aβ affects its aggregation properties and compare it to the effects of other metal ions.

EXPERIMENTAL SECTION

Sample Preparation. Please note that studies were performed in D_2O. However, for clarity, we decided to use the notation pH even if the measurements were made in D_2O. pD was measured using a classical glass electrode according to pD = $pH_{reading}$ + 0.4, and the pD value was corrected according to ref 42 to be in ionization conditions equivalent to those in H_2O.

Human Aβ16 peptide (sequence DAEFRHDSGYEVHHQK), Aβ28 peptide (sequence DAEFRHDSGYEVHHQKLVFFAEDVGSNK), and Aβ40 peptide (sequence DAEFRHDSGYEVHHQKLVFFAEDVGSN KGAIIGLMVGGVV) were bought from GeneCust (Dudelange, Luxembourg).

A stock solution of Aβ16 or Aβ28 peptide was prepared by dissolving the powder in D_2O (resulting pH $\approx$ 2). Peptide concentration was then determined by UV−vis absorption of Tyr10 considered as free tyrosine ($(\varepsilon_{276} - \varepsilon_{296})$ = 1410 $M^{-1}cm^{-1}$). The peptide solutions were then diluted down to the appropriate concentration of Aβ in phosphate buffer. pH was adjusted using $NaOD/D_2SO_4$.

Human Aβ40 peptide was prepared by dissolving the powder in NaOD 0.1 M (resulting pH $\approx$ 13) to give a concentration of approximately 0.5 mM. Peptide concentration was then determined by UV−vis absorption of Tyr10 considered as free tyrosinate ($(\varepsilon_{293} - \varepsilon_{360})$ = 2130 $M^{-1}cm^{-1}$).

Preparation of NMR Samples. Stock solution of Aβ16 or Aβ28 was diluted to 1 (^{1}H NMR), 5 ($^{13}C\{^1H\}$ and 2D experiments of the apo-peptide), or 2 mM ($^{13}C\{^1H\}$ and 2D experiments of the holo-peptide) in 0.2 M phosphate buffer/D_2O at pH 7.2.

For the Aβ40 peptide, the stock solution (pH 13) was then diluted with 0.1 M phosphate buffer (in D_2O and at approximately pH 6.5) and with D_2O to reach a final concentration of 0.2 mM in Aβ40 peptide, 40 mM in phosphate buffer and a final pH of 7.2.

Substoichiometric quantities (ca. 0.1−1.0 equiv) of Fe^{II} from $Fe(NH_4)_2(SO_4)_2$ in D_2O were used.

NMR samples were prepared as follows.

(1) Aβ16 and Aβ28 samples. To a degassed solution of Aβ in 0.2 M phosphate buffer (in D_2O) pH 7.4 (0.7 mL, 1.0 or 2.0 mM) was added a solution of desferrioxamine (DFO) (7 or 70 mM in D_2O, according to Fe concentration) and a freshly prepared solution of $Fe(NH_4)_2(SO_4)_2$ (7 or 70 mM in D_2O) under inert atmosphere. A solution of dithionite (70 or 140 mM in D_2O, 5 equiv) was added to keep Fe into the ferrous state, and the samples were kept under argon in sealed screw-cap NMR tubes. Upon oxidation dithionite forms SO_2 that acidifies the solution. As millimolar peptide concentration and hence 5−10 mM dithionite was used, a strong buffer concentration was necessary to keep the pH constant. Indeed, a stable pH is a prerequisite to evaluate the effect of Fe(II).

A stoichiometric amount with respect to Fe of DFO, a highly selective Fe^{III} chelator, was used to coordinate small amount of Fe^{III} originating from possible partial oxidation of Fe^{II} during long lasting experiments (^{13}C) and avoid its precipitation as iron hydroxide that broadens the signals and reduces the spectral resolution. Comparison of ^{1}H NMR spectra of Aβ16 peptide: DFO:Fe^{III} (1:0.3:0.1) and that of Aβ16 peptide alone shows that no important or selective line broadening is observed, indicating that if there is any interaction between the Fe^{III}−DFO complex and the Aβ16 peptide, it will not perturb detection of the highly specific Fe^{II} to Aβ16 peptide interaction. Moreover, NMR diffusion experiments show that DFO does not interfere with Fe^{II} binding to Aβ (Table S1, Supporting Information). Lastly, we also checked that when dithionite is not added to the solution mixture the effect of Fe^{II} on the Aβ16 ^{1}H NMR signature is similar to that observed in the presence of dithionite. This indicates that interaction of dithionite with Fe^{II} can also be neglected. However, for longer experiments such as ^{13}C experiments the use of added dithionite is required to keep the solution mixture under as strict as possible anaerobic conditions. Note that when x equiv of Fe^{II} is added, x equiv of DFO and 5x of equiv of dithionite are also added. However, for the purpose of clarity, only the Fe^{II} concentration is reported in the figure captions (e.g., 0.3 equiv of Fe^{II} instead of 0.3 equiv of Fe^{II}, 0.3 equiv of DFO, and 1.5 equiv of Fe^{II}).

(2) Aβ40 samples. To avoid degassing the Aβ40 peptide at pH 7.2, which would trigger the aggregation process (due to repetitive freezing/thawing), the Aβ40 stock solution (0.5 mM, pH 13, see above), phosphate buffer, and D_2O were degassed separately and mixed just before the NMR experiment in a Ar-purged sealed screw-cap NMR tube. Note that even if the Aβ40 peptide stock solution is stored at pH 13 and 5 °C, the signal intensity of a newly prepared sample is divided after 48 h by ca. two compared to a sample made with freshly prepared Aβ40 stock solution. The rest of the sample handling is similar to Aβ16 sample.

pH was checked after the NMR experiments and was within the error of the measurement (i.e., ± 0.1 pH unit).

NMR Method. 1D ^{1}H and ^{13}C experiments and 2D experiments were recorded on a Bruker Avance 500 spectrometer equipped with a 5 mm triple-resonance inverse Z-gradient probe (TBI ^{1}H, ^{31}P, BB). All chemical shifts are relative to tetramethylsilane. 1D and 2D NMR spectra were collected at 298 K in D_2O. For the apo-peptide, accumulation lasts ca. 35 h for the $^{13}C\{^1H\}$ NMR experiments and 25 h for the 2D $^1H-^1H$ TOCSY, $^1H-^{13}C$ HSQC, and $^1H-^{13}C$ HMBC experiments. For the holo-peptide, accumulation lasts ca. 72 h for the $^{13}C\{^1H\}$ NMR experiments and 14 h for the 2D $^1H-^1H$ TOCSY and $^1H-^{13}C$ HSQC.

Suppression of the water signal was achieved with WATERGATE or presaturation sequences.

^{1}H NMR spectra were also collected using a Bruker Avance 700 spectrometer equipped with a 5 mm four-channel inverse Z-gradient probe.

Assignments of the ^{1}H and ^{13}C signals: all ^{1}H and ^{13}C signals were assigned on the basis of chemical shifts, spin−spin coupling constants, splitting patterns, and signal intensities and using $^1H-^1H$ TOCSY, $^1H-^{13}C$ HSQC, and $^1H-^{13}C$ HMBC experiments (Table S2, Supporting Information).

ASSOCIATED CONTENT

Supporting Information. ^{1}H and ^{13}C NMR assignments, complementary ^{1}H, ^{13}C, and 2D data are reported in the Supporting Information. This material is available free of charge via the Internet at http://pubs.acs.org.

AUTHOR INFORMATION

Corresponding Author

*Phone: (+33) 5 61 33 31 62 (P.F.), (+33) 5 61 33 31 62 (C.H.). Fax: (+33) 5 61 55 30 03. E-mail: peter.faller@lcc-toulouse.fr (P.F.), christelle.hureau@lcc-toulouse.fr (C.H.),

ACKNOWLEDGMENT

The authors thank the ANR (Agence Nationale de la Recherche) for a postdoctoral fellowship to F.B.-E.G. (ANR Grant Neurometals NT09-488591). Drs. F. Banse (University Paris-Sud, ORSAY) and L. Sabater are acknowledged for fruitful discussions. The authors thank Olivier Saurel for use of the 700 MHz spectrometer.

REFERENCES

(1) Kozlowski, H.; Janicka-Klos, A.; Brasun, J.; Gaggelli, E.; Valensin, D.; Valensin, G. *Coord. Chem. Rev.* **2009**, *253*, 2665–2685.
(2) Smith, M. A.; Harris, P. L.; Sayre, L. M.; Perry, G. *Proc. Natl. Acad. Sci. U.S.A.* **1997**, *94*, 9866–9868.
(3) Lovell, M. A.; Robertson, J. D.; Teesdale, W. J.; Campbell, J. L.; Markesbery, W. R. *J. Neurol. Sci.* **1998**, *158*, 47–52.
(4) Quintana, C.; Bellefqih, S.; Laval, J. Y.; Guerquin-Kern, J. L.; Wu, T. D.; Avila, J.; Ferrer, I.; Arranz, R.; Patiño, C. J. *Struct. Biol.* **2006**, *153*, 42–54.
(5) Grundke-Iqbal, I.; Fleming, J.; Tung, Y. C.; Lassmann, H.; Iqbal, K.; Joshi, J. G. *Acta Neuropathol.* **1990**, *81*, 105–110.
(6) Meadowcroft, M. D.; Connor, J. R.; Smith, M. B.; Yang, Q. X. *J. Magn. Reson. Imaging* **2009**, *29*, 997–1007.
(7) Casadesus, G.; Smith, M. A.; Zhu, X.; Aliev, G.; Cash, A. D.; Honda, K.; Petersen, R. B.; Perry, G. *J. Alzheimers Dis.* **2004**, *6*, 165–169.
(8) Smith, M. A.; Zhu, X.; Tabaton, M.; Liu, G.; McKeel, D. W. J.; Cohen, M. L.; Wang, X.; Siedlak, S. L.; Dwyer, B. E.; Hayashi, T.; Nakamura, M.; Nunomura, A.; Perry, G. *J. Alzheimers Dis.* **2010**, *19*, 363–372.
(9) Bishop, G. M.; Robinson, S. R. *J. Neurosci. Res.* **2003**, *73*, 316–323.
(10) Liu, B.; Moloney, A.; Meehan, S.; Morris, K.; Thomas, S. E.; Serpell, L. C.; Hider, R.; Marciniak, S. J.; Lomas, D. A.; Crowther, D. C. *J. Biol. Chem.* **2011**, *286*, 4248–4256.
(11) Mantyh, P. W.; Ghilardi, J. R.; Rogers, S.; DeMaster, E.; Allen, C. J.; Stimson, E. R.; Maggio, J. E. *J. Neurochem.* **1993**, *61*, 1171–1174.
(12) Rogers, J. T.; Bush, A. I.; Cho, H. H.; Smith, D. H.; Thomson, A. M.; Friedlich, A. L.; Lahiri, D. K.; Leedman, P. J.; Huang, X.; Cahill, C. M. *Biochem. Soc. Trans.* **2008**, *36*, 1282–1287.
(13) Silvestri, L.; Camaschella, C. *J. Cell. Mol. Med.* **2008**, *12*, 1548–1550.
(14) Duce, J. A.; Tsatsanis, A.; Cater, M. A.; James, S. A.; Robb, E.; Wikhe, K.; Leong, S. L.; Perez, K.; Johanssen, T.; Greenough, M. A.; Cho, H. H.; Galatis, D.; Moir, R. D.; Masters, C. L.; McLean, C.; Tanzi, R. E.; Cappai, R.; Barnham, K. J.; Ciccotosto, G. D.; Rogers, J. T.; Bush, A. I. *Cell* **2010**, *142*, 857–867.
(15) Mandel, S.; Amit, T.; Bar-Am, O.; Youdim, M. B. *Prog. Neurobiol.* **2007**, *82*, 348–360.
(16) Faller, P.; Hureau, C. *Dalton Trans.* **2009**, 1080–1094.
(17) Karr, J. W.; Kaupp, L. J.; Szalai, V. A. *J. Am. Chem. Soc.* **2004**, *126*, 13534–13538.
(18) Minicozzi, V.; Stellato, F.; Comai, M.; Dalla Serra, M.; Potrich, C.; Meyer-Klaucke, W.; Morante, S. *J. Biol. Chem.* **2008**, *283*, 10784–10792.
(19) Syme, C. D.; Nadal, R. C.; Rigby, S. E.; Viles, J. H. *J. Biol. Chem.* **2004**, *279*, 18169–18177.
(20) Dorlet, P.; Gambarelli, S.; Faller, P.; Hureau, C. *Angew. Chem., Int. Ed.* **2009**, *48*, 9273–9276.
(21) Drew, S. C.; Noble, C. J.; Masters, C. L.; Hanson, G. R.; Barnham, K. J. *J. Am. Chem. Soc.* **2009**, *131*, 1195–1207.
(22) Hureau, C.; Balland, V.; Coppel, Y.; Solari, P. L.; Fonda, E.; Faller, P. *J. Biol. Inorg. Chem.* **2009**, 995–1000.
(23) Shearer, J.; Szalai, V. A. *J. Am. Chem. Soc.* **2008**, *130*, 17826–17835.
(24) Danielsson, J.; Pierattelli, R.; Banci, L.; Graslund, A. *FEBS J.* **2007**, *274*, 46–59.
(25) Hou, L.; Zagorski, M. G. *J. Am. Chem. Soc.* **2006**, *128*, 9260–9261.
(26) Hureau, C.; Coppel, Y.; Dorlet, P.; Solari, P. L.; Sayen, S.; Guillon, E.; Sabater, L.; Faller, P. *Angew. Chem., Int. Ed.* **2009**, *48*, 9522–9525.
(27) Eury, H.; Bijani, C.; Faller, P.; Hureau, C. *Angew. Chem., Int. Ed.* **2011**, *50*, 901–905.
(28) Exley, C. *J. Alzheimers Dis.* **2006**, *10*, 173–177.
(29) House, E.; Collingwood, J.; Khan, A.; Korchazkina, O.; Berthon, G.; Exley, C. *J. Alzheimers Dis.* **2004**, *6*, 291–301.
(30) Baruch-Suchodolsky, R.; Fischer, B. *Biochemistry* **2008**, *47*, 7796–7806.
(31) Khan, A.; Dobson, J. P.; Exley, C. *Free Radical Biol. Med.* **2006**, *40*, 557–569.
(32) Jiang, D.; Li, X.; Williams, R.; Patel, S.; Men, L.; Wang, Y.; Zhou, F. *Biochemistry* **2009**, *48*, 7939–7947.
(33) Cui, Q.; Thorgersen, M. P.; Westler, W. M.; Markley, J. L.; Downs, D. M. *Proteins* **2006**, *62*, 578–586.
(34) He, Y. N.; Alam, S. L.; Proteasa, S. V.; Zhang, Y.; Lesuisse, E.; Dancis, A.; Stemmler, T. L. *Biochemistry* **2004**, *43*, 16254–16262.
(35) Rai, P.; Wemmer, D. E.; Linn, S. *Nucleic Acids Res.* **2005**, *33*, 497–510.
(36) Bhattacharya, S.; Lecomte, J. T. *Biophys. J.* **1997**, *73*, 3241–3156.
(37) Gaggelli, E.; Kozlowski, H.; Valensin, D.; Valensin, G. *Chem. Rev.* **2006**, *106*, 1995–2044.
(38) Gaggelli, E.; D'Amelio, N.; Valensin, D.; Valensin, D. *Magn. Reson. Chem.* **2003**, *41*, 877–883.
(39) Mekmouche, Y.; Coppel, Y.; Hochgrafe, K.; Guilloreau, L.; Talmard, C.; Mazarguil, H.; Faller, P. *ChemBioChem* **2005**, *6*, 1663–1671.
(40) Drew, S. C.; Masters, C. L.; Barnham, K. J. *J. Am. Chem. Soc.* **2009**, *131*, 8760–8761.
(41) Opazo, C.; Huang, X.; Cherny, R. A.; Moir, R. D.; Roher, A. E.; White, A. R.; Cappai, R.; Masters, C. L.; Tanzi, R. E.; Inestrosa, N. C.; Bush, A. I. *J. Biol. Chem.* **2002**, *277*, 40302–40308.
(42) Delgado, R.; Da Silva, J. J. R. F.; Amorim, M. T. S.; Cabral, M. F.; Chaves, S.; Costa, J. *Anal. Chim. Acta* **1991**, *245*, 271–282.